

**Vedran Mrzljak**

E-mail: vedran.mrzljak@riteh.hr

**Jasna Prpić-Oršić**

E-mail: jasna.prpic-orsic@riteh.hr

University of Rijeka, Faculty of Engineering, Vukovarska 58, 51000 Rijeka, Croatia,

**Igor Poljak**

E-mail: igor.poljak2@gmail.com

Rožići 4/3, 51221 Kostrena, Croatia

---

## **Energy Power Losses and Efficiency of Low Power Steam Turbine for the Main Feed Water Pump Drive in the Marine Steam Propulsion System**

### **Abstract**

Steam turbine for the main feed water pump (MFP) drive is a low power turbine, for which energy power losses and energy efficiency analysis are presented in this paper. The MFP steam turbine analysis has been performed within a wide range of turbine loads. The influence of steam specific entropy increment of the real (polytropic) steam expansion upon the MFP turbine energy power losses and energy efficiency has been investigated. During all the observed loads MFP steam turbine energy power losses were in the range between 346.2 kW and 411.4 kW. The MFP steam turbine energy power losses and energy efficiency were most significantly influenced by the steam specific entropy increment. Change in the steam specific entropy increment is directly proportional to the change in MFP turbine energy power losses, while the change in the steam specific entropy increment is reversely proportional to the MFP turbine energy efficiency change. For the observed turbine loads, the MFP steam turbine energy efficiency was in the range between 46.83% and 51.01%.

**Key words:** Low power steam turbine, Energy efficiency, Energy power losses, Marine steam system

### **1. Introduction**

Steam propulsion plants can be found nowadays in most LNG carriers [1]. A steam propulsion plant consists of a series of components [2]. One of them is the low power steam turbine for the Main Feed Water Pump (MFP) drive. The MFP steam turbine has been analyzed in this paper from the aspect of energy, for a number of propulsion system loads.

The MFP low power steam turbine has a single Curtis stage. Steam turbines with Curtis and other known stages along with their complete analysis can be found in literature [3] and [4]. Many details of both classic and special designs of marine steam turbines and their auxiliary systems are presented in [5] and [6].

The MFP steam turbine analysis objective is to determine the specific entropy increment change during steam expansion from the real ship exploitation under different steam turbine loads. Growth of the steam specific entropy increment usually indicates increased steam turbine energy power losses, although this does not have to be the rule. This analysis dealt with the influence of the steam specific entropy increment change on MFP steam turbine energy power losses and energy efficiency change, at each observed operating point.

## 2. Steam turbine energy analysis

### 2.1. Energy analysis - general equations

Energy analysis is based on the first law of thermodynamics [7]. Mass and energy balance equations for a standard volume in steady state can be expressed according to [8] as:

$$\sum \dot{m}_{\text{IN}} = \sum \dot{m}_{\text{OUT}} \quad (1)$$

$$\dot{Q} - P = \sum \dot{m}_{\text{OUT}} \cdot h_{\text{OUT}} - \sum \dot{m}_{\text{IN}} \cdot h_{\text{IN}} \quad (2)$$

Energy power of a flow can be calculated according to the equation [9]:

$$\dot{E}_{\text{en}} = \dot{m} \cdot h \quad (3)$$

Energy efficiency can be calculated according to [10] as:

$$\eta_{\text{en}} = \frac{\text{Energy output}}{\text{Energy input}} \quad (4)$$

### 2.2. MFP steam turbine energy efficiency and energy power losses

Low power steam turbine, which drives the main feed water pump, is traditionally used in LNG carriers with steam propulsion. The main feed water pump (MFP) is used for increasing water pressure and returning it to steam generators. The analyzed MFP steam turbine consists of one Curtis stage, while the whole unit has the following characteristics [11]:

- Pump delivery height: 818 m
- Pump maximum capacity: 175 m<sup>3</sup>/h
- Steam turbine maximum power: 570 kW

Figure 1 presents the steam mass flow through the MFP steam turbine along with specific enthalpy and specific entropy at the steam turbine inlet and outlet. An important operating parameter measured for every load, which will be used to calculate the real developed power of the MFP steam turbine, is the main feed water pump volume flow (capacity) also presented in Figure 1.

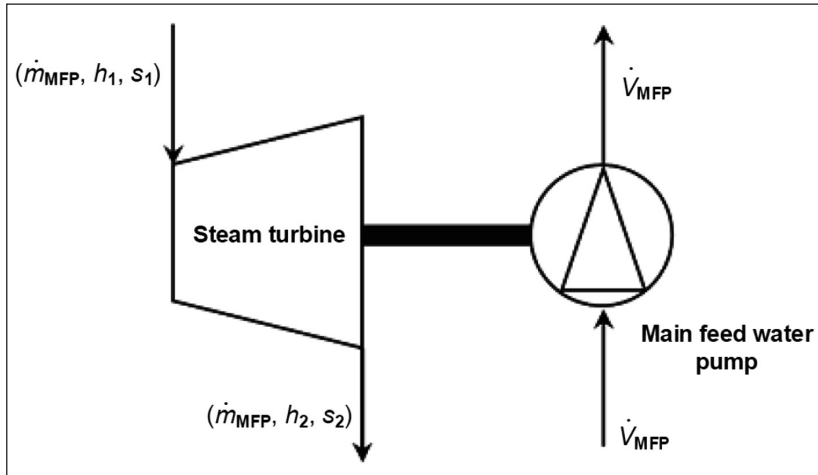


Figure 1 - Change in main operating parameters through the MFP steam turbine and main feed water pump

The MFP steam turbine real developed power was approximated against the main feed water pump volume flow  $\dot{V}_{MFP}$  by using third degree polynomial (5), according to producer specifications [11]. The main feed water pump volume flow in relation to the MFP steam turbine real developed power was calculated for medium water density  $\rho_{fw} = 937.48 \text{ kg/m}^3$  at water temperature of  $T_{fw} = 127 \text{ }^\circ\text{C}$ , according to producer recommendations, Figure 2. The MFP steam turbine real developed power was calculated as:

$$P_{MFP,RE} = 1.78582 \cdot 10^{-5} \cdot \dot{V}_{MFP}^3 - 3.08892 \cdot 10^{-3} \cdot \dot{V}_{MFP}^2 + 2.002 \cdot \dot{V}_{MFP} + 189.48 \quad (5)$$

where  $P_{MFP,RE}$  is obtained in (kW) when  $\dot{V}_{MFP}$  is inserted in the equation (5) in ( $\text{m}^3/\text{h}$ ).

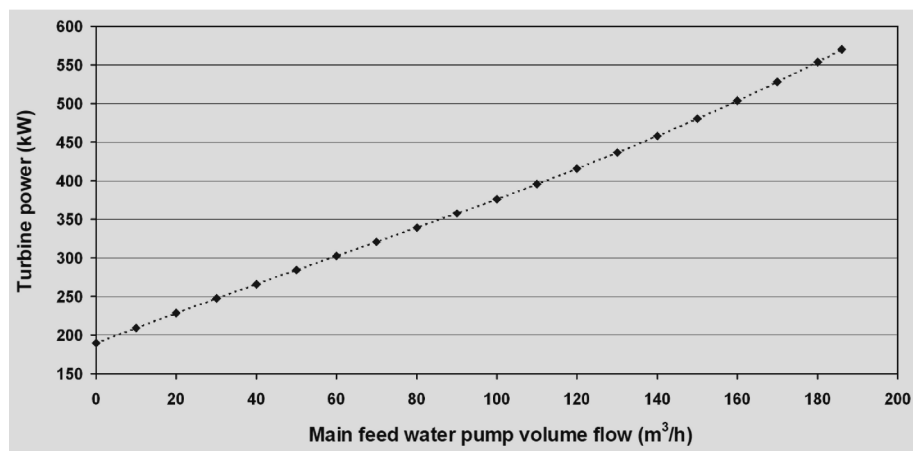


Figure 2 - The MFP steam turbine real developed power in relation to the main feed water pump volume flow [11]

The steam mass flow through the MFP steam turbine was approximated with the main feed water pump real power demand  $P_{\text{MFP,RE}}$ , Figure 3 Approximation was made according to producer specifications [11] by using third degree polynomial:

$$\dot{m}_{\text{MFP}} = -3 \cdot 10^{-5} \cdot P_{\text{MFP,RE}}^3 + 3.1326 \cdot 10^{-2} \cdot P_{\text{MFP,RE}}^2 - 4.396794 \cdot P_{\text{MFP,RE}} + 2386.60 \quad (6)$$

where  $\dot{m}_{\text{MFP}}$  is obtained in kg/h when  $P_{\text{MFP,RE}}$  in (kW) is placed in the equation (6).

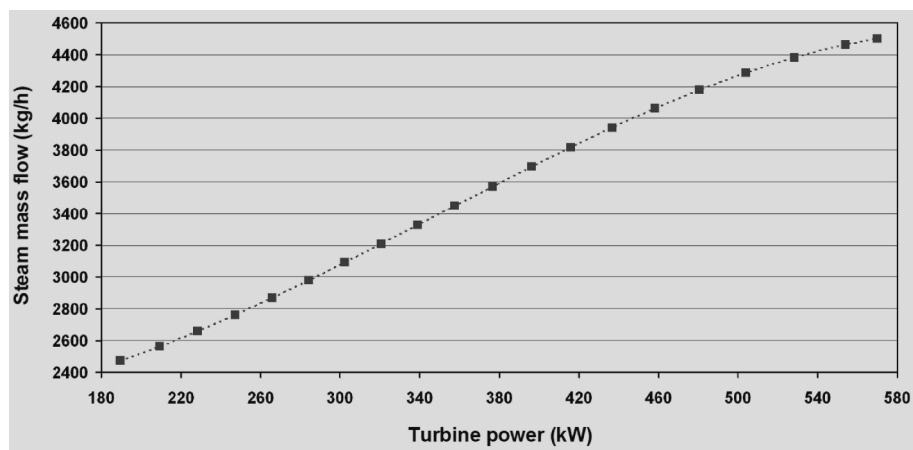


Figure 3 - The MFP turbine steam mass flow in relation to the turbine real developed power [11]

As there was no leakage recorded in the analyzed MFP steam turbine, the steam mass flow balance for the MFP turbine inlet and outlet was:

$$\dot{m}_{\text{MFP},1} = \dot{m}_{\text{MFP},2} = \dot{m}_{\text{MFP}} \quad (7)$$

According to Figure 1 and Figure 4,  $h_1$  is the steam specific enthalpy at the turbine inlet and  $h_2$  is the steam specific enthalpy at the turbine outlet after real (polytropic) expansion. The steam specific enthalpy at the turbine inlet  $h_1$  as well as the steam specific entropy at the turbine inlet  $s_1$  was calculated from the measured steam pressure and temperature at the turbine inlet. The steam real specific enthalpy at the turbine outlet  $h_2$  was calculated from the real MFP turbine developed power  $P_{\text{MFP,RE}}$  in (kW) and from the steam mass flow  $\dot{m}_{\text{MFP}}$  in (kg/s) according to [12] by equation:

$$h_2 = h_1 - \frac{P_{\text{MFP,RE}}}{\dot{m}_{\text{MFP}}} \quad (8)$$

The steam real specific entropy at the turbine outlet  $s_2$  was calculated from the steam real specific enthalpy at the turbine outlet  $h_2$  and measured pressure at the turbine outlet  $p_2$ .

Specific enthalpy after isentropic steam expansion  $h_{2S}$  was calculated from the measured steam pressure at the turbine outlet  $p_2$  and from the known steam specific entropy at the turbine inlet  $s_1$ . The ideal isentropic expansion assumes no change in the steam specific entropy ( $s_1 = s_{2S}$ ), Figure 4.

The steam specific enthalpy at the turbine inlet  $h_1$ , steam specific enthalpy at the end of the isentropic expansion  $h_{2S}$  and both steam specific entropies (at the turbine inlet  $s_1$  and outlet  $s_2$ ) were calculated by using NIST REFPROP 8.0 software [13].

In order for a proper description of MFP steam turbine energy power losses, the real turbine developed power and isentropic power must be known, which can be developed in the ideal situation (where change in the steam specific entropy does not occur). The isentropic MFP steam turbine power, according to Figure 4, is to be calculated as:

$$P_{\text{MFP,IS}} = \dot{m}_{\text{MFP}} \cdot (h_1 - h_{2S}) \quad (9)$$

MFP steam turbine energy power losses can be calculated by using the following equation:

$$\dot{E}_{\text{MFP,en,PL}} = P_{\text{MFP,IS}} - P_{\text{MFP,RE}} = \dot{m}_{\text{MFP}} \cdot (h_2 - h_{2S}) \quad (10)$$

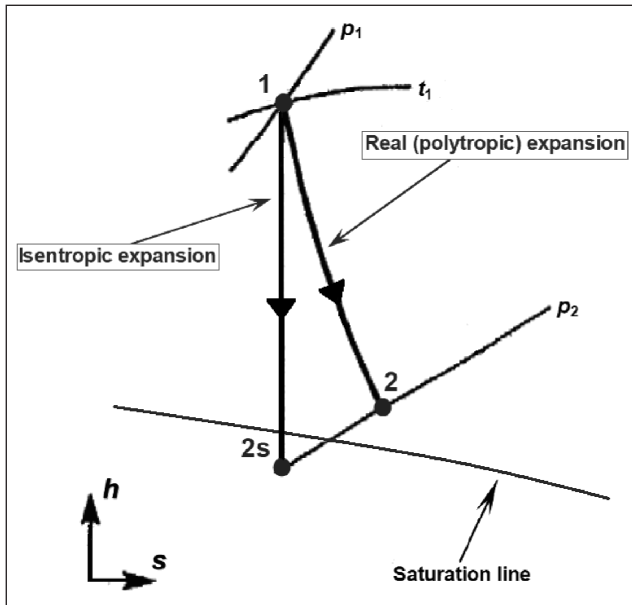


Figure 4 - The MFP steam turbine real (polytropic) and ideal (isentropic) expansion

Energy efficiency of the MFP steam turbine can be calculated according to [14] by using the equation:

$$\eta_{MFP,en} = \frac{(h_1 - h_2)}{(h_1 - h_{2s})} = \frac{P_{MFP,RE}}{P_{MFP,IS}} \tag{11}$$

### 3. The MFP steam turbine measuring equipment and measurement results

Measurement results for required operating parameters for the MFP steam turbine are presented in relation to the propulsion propeller speed, Table 1. The propulsion propeller speed is directly proportional to the MFP steam turbine load, i.e. a higher propulsion propeller speed denotes a higher steam turbine load.

*Table 1 - MFP steam turbine measurement results in various operation regimes*

Operating point	Propulsion propeller speed (rpm)	Steam pressure at the MFP turbine inlet (MPa)	Steam temperature at the MFP turbine inlet (°C)	Steam pressure at the MFP turbine outlet (MPa)	MFP feed water volume flow (m <sup>3</sup> /h)
1	25.00	6.207	485	0.272	74.49
2	41.78	6.215	488	0.270	75.08
3	56.65	5.972	496	0.276	84.48
4	65.10	6.074	502	0.266	76.64
5	68.66	6.067	510	0.251	82.90
6	71.03	6.078	511	0.237	87.29
7	76.56	6.010	512	0.256	100.52
8	79.46	5.874	510	0.235	106.01
9	82.88	5.795	500	0.250	117.04

Measurement results were obtained from the existing measuring equipment mounted at the MFP steam turbine inlet and outlet and at the main feed water pump inlet. The list of measuring equipment used was presented in Table 2.

*Table 2 - Equipment for the MFP steam turbine and main feed water pump measurements*

Steam temperature (MFP turbine inlet)	Greisinger GTF 601-Pt100 - Immersion probe [15]
Steam pressure (MFP turbine inlet)	Yamatake JTG980A - Pressure Transmitter [16]
Steam pressure (MFP turbine outlet)	Yamatake JTG940A - Pressure Transmitter [16]
Feed water volume flow (pump inlet)	Promass 80F - Coriolis Mass Flow Measuring System [17]
Propulsion propeller speed	Kyma Shaft Power Meter (KPM-PFS) [18]

The analysis was carried out using the steam pressure and temperature at the MFP turbine inlet, before governing valves. Before coming to the first turbine stage, the steam passes through a set of governing valves positioned in the turbine steam chest. The governing valves operating principle is to reduce steam pressure and temperature while the steam specific enthalpy remains constant. Governing valves operation is most intense at low steam turbine loads.

The MFP steam turbine belonging to the analyzed LNG carrier is not provided with the required measuring equipment in the steam chest (to obtain precise steam operating parameters) and therefore the analysis was carried out with a steam pressure and temperature at the steam chest inlet. The only data available for steam temperature and pressure for the analyzed turbine steam chest, for several turbine loads, were found by the authors in producer specifications during turbine testing [11]. These data have not been included in the presented analysis because they were not measured during any actual exploitation of the LNG carrier propulsion plant and may significantly depart from real exploitation data.

According to producer test data, an analysis of the impact the steam chest pressure and temperature change produce upon the calculated operating parameters was carried out. Change in the steam chest pressure and temperature influenced the turbine energy efficiency and specific entropy values up to 5% on the average for all turbine operating points observed.

Significant differences (up to 20% on the average) can only be expected in turbine energy power loss values. Small changes in the steam specific enthalpy at the turbine outlet multiplied by the steam mass flow, equation (10), is the main reason for these significant differences.

#### **4. MFP steam turbine energy analysis results with the discussion**

The steam specific entropy difference (increment) between the inlet and outlet of the MFP steam turbine is presented in Figure 5 for all the observed steam turbine loads. While the steam specific entropy at the MFP steam turbine inlet for lowest loads amounts approximately to  $6.8 \text{ kJ/kg}\cdot\text{K}$ , at the propulsion propeller speed of 56.65 rpm it is increased to  $6.9 \text{ kJ/kg}\cdot\text{K}$  and keeps approximately the same value until the highest observed loads are involved. The steam specific entropy at the MFP turbine outlet records much more intense changes during the whole range of loads observed, Figure 5, and therefore the steam specific entropy increment will be most influenced by the steam specific entropy at the MFP turbine outlet.

As presented in Figure 5, the MFP steam turbine steam specific entropy increment change does not show any continuous trend following the increase in the steam system load. The lowest values of the steam specific entropy increment ( $0.82 \text{ kJ/kg}\cdot\text{K}$ ) can be noticed at propulsion propeller speeds of 56.65 rpm and 82.88 rpm while the highest value of steam specific entropy increment is  $0.91 \text{ kJ/kg}\cdot\text{K}$  at 71.03 rpm.

Increase in the steam specific entropy increment usually indicates an increase in the system energy power losses in a large number of different systems [14]. This analysis will investigate whether the same conclusion applies for the MFP steam turbine.

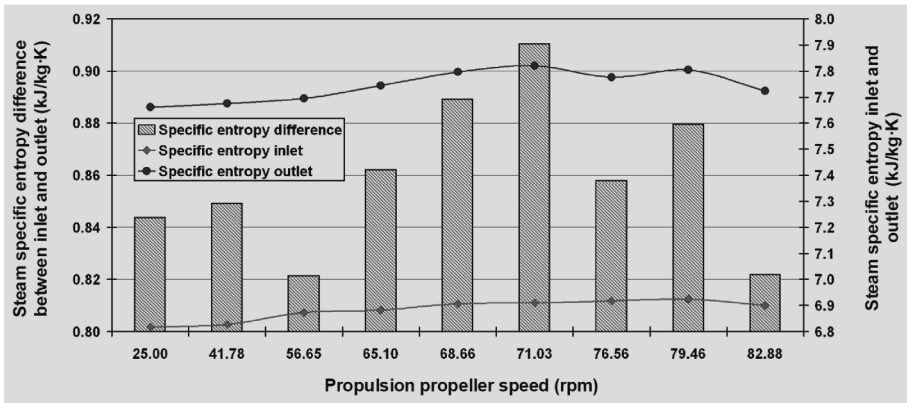


Figure 5 - Steam specific entropy change at the MFP steam turbine inlet and outlet along with specific entropy difference (increment) between inlet and outlet

Figure 6 presents the MFP turbine (MFPT) isentropic and real power change. The isentropic MFP turbine power can theoretically be developed by using real operating parameters, yet without any losses (with no change in the steam specific entropy, according to Figure 4). The MFP turbine real power is the one developed according to real operating parameters measured in the propulsion system during navigation.

The MFP turbine real power was calculated according to equation (5) while the isentropic power was calculated according to equation (9). Within the whole range of propulsion propeller speeds observed, the isentropic MFP steam turbine power varied from 675.2 kW up to 803.8 kW, while in the same load range the real MFP turbine power varied from 329 kW up to 410 kW. The maximum real power of the MFP steam turbine according to producer specifications is 570 kW. The ideal (isentropic) steam expansion for the observed steam turbine loads results in power values exceeding the maximum real power that can be developed.

The real MFP turbine power depends on the current feed water volume flow through the main pump. As can be seen in Figure 6, an increase in the steam system load (increase in the propulsion propeller speed) will result in an increase in the feed water volume flow through the main pump and further in an increase in the real MFP turbine power. Trend lines of the real and isentropic MFP turbine developed power must be the same, as presented in Figure 6.

The difference in the isentropic and real MFP steam turbine power represents energy power losses of the real MFP turbine steam expansion process as compared with the ideal one.

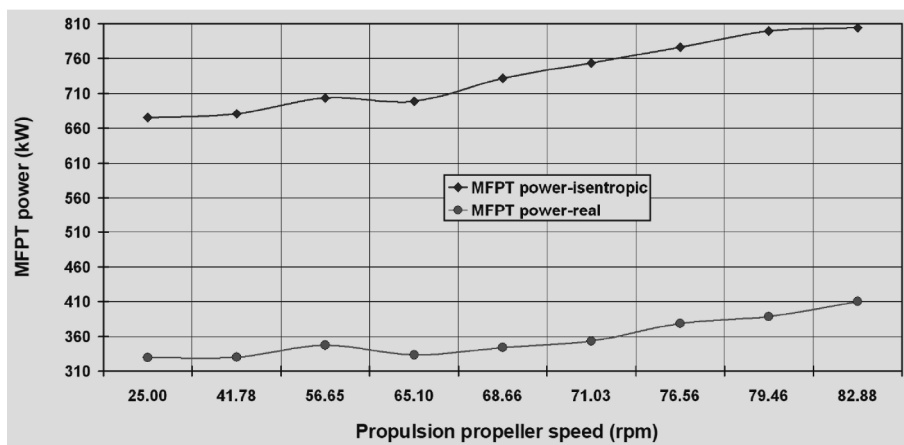


Figure 6 - Change in the MFP steam turbine power (real and isentropic) for observed steam system loads

An increase in the steam specific entropy increment reduces the available steam specific enthalpy difference which will be used in steam turbine. As a result, an increase in the steam specific entropy increment will cause a decrease in the real developed steam turbine power.

As can be seen in Figure 5 and Figure 7, the change in MFP steam turbine specific entropy increment has the most significant influence on the change in the MFP steam turbine energy power losses. When each two propulsion propeller speeds are compared, the change in the steam specific entropy increment results directly proportional to the change in the MFP steam turbine energy power losses. During the increase in the steam specific entropy increment, the MFP steam turbine energy power losses are also increased and vice versa for all observed propulsion propeller speeds except 41.78 rpm and 56.65 rpm.

At the propulsion propeller speed of 41.78 rpm, the steam specific entropy increment amounts to 0.85 kJ/kg·K to decrease thereafter to 0.82 kJ/kg·K at 56.65 rpm, Figure 5. At the same time, the MFP steam turbine energy power losses increase, Figure 7. The reason why the MFP turbine energy power losses increase, regardless of the decrease in the steam specific entropy increment, is the feed water volume flow increase from 75.08 m<sup>3</sup>/h (41.78 rpm) to 84.48 m<sup>3</sup>/h (56.65 rpm), Table 1. The change in the feed water volume flow is also directly proportional to the change in the MFP steam turbine energy power losses. The increase in the feed water volume flow increases the MFP steam turbine energy power losses and vice versa.

It can be concluded that the most significant influence on the MFP steam turbine energy power losses is produced by the steam specific entropy increment and in some situations, between some propulsion propeller speeds, the dominant influence on the change in the MFP steam turbine energy power losses can be produced by a feed water

volume flow sensible change as well.

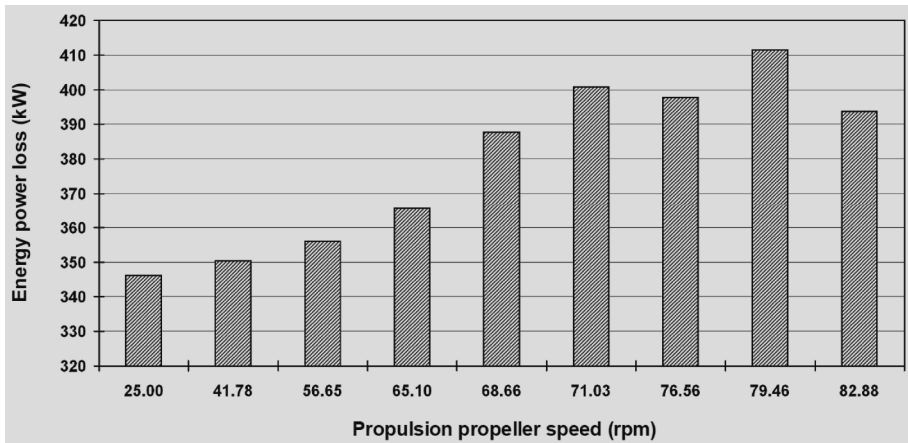


Figure 7 - The MFP steam turbine energy power loss change for the observed steam system loads

Steam specific entropy increment can be used as an essential parameter for the evaluation of the MFP steam turbine energy efficiency change. The steam specific entropy increment change is reversely proportional to the MFP steam turbine energy efficiency change for all observed steam system loads. During the increase in the steam specific entropy increment, the MFP turbine energy efficiency decreases and during the decrease in the steam specific entropy increment, the MFP turbine energy efficiency increases, Figure 5 and Figure 8.

The highest MFP steam turbine energy efficiency of 51.01 % was obtained at the lowest steam specific entropy increment of 0.82 kJ/kg·K at the propulsion propeller speed of 82.88 rpm, Figure 8. The lowest MFP steam turbine energy efficiency of 46.83 % was obtained for the highest steam specific entropy increment of 0.91 kJ/kg·K at the propulsion propeller speed of 71.03 rpm.

The analyzed MFP steam turbine is a low power steam turbine with real maximum power of 570 kW. Its energy efficiency, for the observed loads, ranges from 46.83 % to 51.01 %, representing an expected range of energy efficiency for the low power steam turbine in general [9].

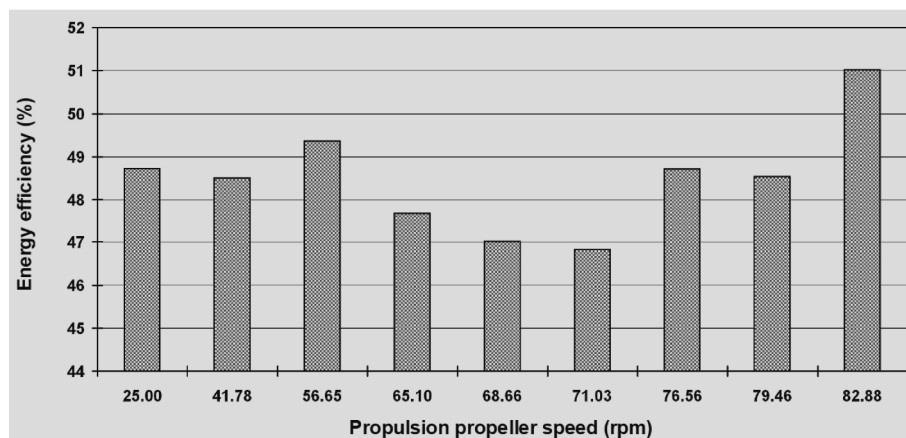


Figure 8 - The MFP steam turbine energy efficiency change for the observed steam system loads

## Conclusions

An analysis of energy efficiency and energy power losses for low power steam turbine, in a wide range of turbine loads, has been presented in this paper. The analysis dealt with the influence of the steam specific entropy increment produced in the real (polytropic) expansion process upon energy power losses and energy efficiency of the MFP steam turbine.

The MFP steam turbine energy power losses were calculated as a difference between the steam turbine real developed power (polytropic steam expansion) and the power which can develop in an ideal situation without any specific entropy increment (isentropic steam expansion). The MFP turbine energy power losses, for the loads observed, were in the range from 346.2 kW to 411.4 kW. The most significant influence on the MFP steam turbine energy power losses is produced by the steam specific entropy increment. It was shown in several cases, between some of the MFP steam turbine loads, that the dominant influence on the change in the turbine energy power losses can also be produced by a sensible change in the feed water volume flow. Change in the steam specific entropy increment and change in the feed water volume flow are directly proportional to the change in the MFP steam turbine energy power losses.

Change in the steam specific entropy increment can also be used to estimate the change in the MFP steam turbine energy efficiency. The steam specific entropy increment change is reversely proportional to the MFP steam turbine energy efficiency change. Increase in the steam specific entropy increment resulted in a decrease in the MFP turbine energy efficiency and vice versa. The presented conclusion is valid for the complete steam system load range observed. The MFP steam turbine energy efficiency

ranges from 46.83 % to 51.01 %, that represents an expected range of energy efficiency for the analyzed low power steam turbine.

## Acknowledgment

Authors' thanks and appreciation go to the ship-owner's head office for the conceded measuring equipment and for the assistance extended during exploitation measurements. The work was supported by the University of Rijeka (Contract No. 13.09.1.1.05) and the Croatian Science Foundation - Project 8722.

### NOMENCLATURE

#### Abbreviations:

LNG Liquefied Natural Gas

MFP Main Feed Water Pump

#### Latin Symbols:

$\dot{E}$  stream flow power, kJ/s

$h$  specific enthalpy, kJ/kg

$\dot{m}$  mass flow, kg/s or kg/h

$p$  pressure, MPa

$P$  power, kW

$\dot{Q}$  heat transfer, kJ/s

$s$  specific entropy, kJ/kg·K

$T$  temperature, °C

$\dot{V}$  volume flow, m<sup>3</sup>/h

#### Greek symbols:

$\rho$  density, kg/m<sup>3</sup>

$\eta$  efficiency, -

#### Subscripts:

en energy

fw feed water

IN inlet

IS isentropic (ideal)

OUT outlet

PL power loss

RE real

## References

1. Schinas, O., Butler, M.: *Feasibility and Commercial Considerations of LNG-fueled Ships*, Ocean Engineering 122, p. 84–96, 2016. (doi:10.1016/j.oceaneng.2016.04.031).
2. Fernández, I. A., Gómez, M. R., Gómez, J. R., Insua, A. A. B.: *Review of Propulsion Systems on LNG Carriers*, Renewable and Sustainable Energy Reviews 67, p. 1395–1411, 2017. (doi:10.1016/j.rser.2016.09.095).
3. Bloch, H. P., Singh, M. P.: *Steam Turbines - Design, Applications and Re-rating*, 2<sup>nd</sup> edition, The McGraw-Hill Companies, Inc., 2009.
4. Sarkar, D. K.: *Thermal Power Plant - Design and Operation*, Elsevier Inc., 2015.
5. Baldi, F., Ahlgren, F., Melino, F., Gabriellini, C., Andersson, K.: *Optimal Load Allocation of Complex Ship Power Plants*, Energy Conversion and Management 124, p. 344–356, 2016. (doi:10.1016/j.enconman.2016.07.009).
6. Haglind, F.: *Variable Geometry Gas Turbines for Improving the Part-load Performance of Marine Combined Cycles - Combined Cycle Performance*, Applied Thermal Engineering 31, p. 467–476, 2011 (doi:10.1016/j.applthermaleng.2010.09.029).
7. Kaushik, S. C., Siva Reddy, V., Tyagi, S. K.: *Energy And Exergy Analyses of Thermal Power Plants: A Review*, Renewable and Sustainable Energy Reviews 15, p. 1857–1872, 2011. (doi:10.1016/j.rser.2010.12.007).
8. Hafdhi, F., Khir, T., Ben Yahyia, A., Ben Brahim, A.: *Energetic and Exergetic Analysis of a Steam Turbine Power Plant in an Existing Phosphoric Acid Factory*, Energy Conversion and Management 106, p. 1230–1241, 2015. (doi:10.1016/j.enconman.2015.10.044).
9. Mrzljak, V., Poljak, I., Mrakovčić, T.: *Energy and Exergy Analysis of the Turbo-generators and Steam Turbine for the Main Feed Water Pump Drive on LNG Carrier*, Energy Conversion and Management 140, p. 307–323, 2017. (doi:10.1016/j.enconman.2017.03.007).
10. Mrzljak, V., Poljak, I., Medica-Viola, V.: *Dual Fuel Consumption and Efficiency of Marine Steam Generators for the Propulsion of LNG Carrier*, Applied Thermal Engineering 119, p. 331–346, 2017. (doi:10.1016/j.applthermaleng.2017.03.078).
11. *Final Drawing for Main Feed Pump & Turbine*, Shinko Ind. Ltd., Hiroshima, Japan, 2006., internal ship documentation.
12. Ahmadi, G., Toghraie, D., Azimian, A., Akbari, O. A.: *Evaluation of Synchronous Execution of Full Repowering and Solar Assisting in a 200 MW Steam Power Plant, a case study*, Applied Thermal Engineering 112, p. 111–123, 2017. (doi:10.1016/j.applthermaleng.2016.10.083).
13. Lemmon, E.W., Huber, M.L., McLinden, M.O.: *NIST Reference Fluid Thermodynamic and Transport Properties-REFPROP*, version 8.0, User's guide, Colorado, 2007.
14. Kanoğlu, M., Çengel, Y.A., Dincer, I.: *Efficiency Evaluation of Energy Systems*, Springer Briefs in Energy, Springer, 2012. (doi:10.1007/978-1-4614-2242-6).
15. <https://www.greisinger.de>, (accessed 15.07.17).
16. <http://www.industriascontrolpro.com>, (accessed 15.07.17).
17. <https://portal.endress.com>, (accessed 15.07.17).
18. <https://www.kyma.no>, (accessed 15.07.17).

Vedran Mrzljak, Igor Poljak, Jasna Prpić-Oršić

## **Energijska učinkovitost i gubici parne turbine male snage za pogon glavne napojne pumpe u brodskom parnoturbinskom postrojenju**

### **Sažetak**

Parna turbina za pogon glavne napojne pumpe (GNP) je turbina male snage, čija energijska učinkovitost i energijski gubici predstavljaju predmet analize u ovom radu. Analiza GNP parne turbine provedena je u širokom rasponu radnih opterećenja. Istražen je utjecaj prirasta specifične entropije pare realne (politropske) ekspanzije na energijske gubitke i učinkovitosti GNP parne turbine. Energijski gubici GNP parne turbine na svim promatranim opterećenjima kreću se u rasponu od 346.2 kW do 411.4 kW. Najznačajniji utjecaj na energijsku učinkovitost i energijske gubitke GNP turbine ima prirast specifične entropije pare. Promjena prirasta specifične entropije pare direktno je proporcionalna promjeni energijskih gubitaka GNP parne turbine, a obrnuto je proporcionalna promjeni energijske učinkovitosti. Za promatrana opterećenja, energijska učinkovitost analizirane turbine kretala se u rasponu od 46.83 % do 51.01 %.

**Ključne riječi:** parna turbina male snage, energijska učinkovitost, energijski gubici, brodska propulzija

